Design of a forearm rehabilitation robot

Pin-Cheng Kung, Ming-Shaung Ju, Chou-Ching K. Lin

Abstract—**A robot intended for assisting forearm rehabilitation of patients with neuromuscular disorders was designed. The robot can guide subject's forearm to pronate/supinate along planned seesaw-like or ramp-and-hold trajectories under a passive mode or an active mode. Preliminary tests on three normal subjects revealed that the robot could, in passive mode, guide the relaxed forearm of subjects to move in the planned trajectory and, in active mode, apply a specified torque on the forearm during voluntary movement.**

I. INTRODUCTION

Rehabilitation program is the main stay of treatment for patients suffering from trauma, stroke or spinal cord injury. Conventionally, these programs rely heavily on the experience and manual manipulation by the therapists on the patients' affected limbs. Since the number of patients is large and the treatment is time-consuming, it is a great advance if robots can assist in performing treatments. Recently have been many researches working on how to use robots in assisting patients in rehabilitation. Lum *et al.* [1] developed a mirror image movement enabler (MIME) system. A six degree-of-freedom robot was used to implement bilateral exercises and it allowed the intact arm to guide therapy of the impaired arm. Krebs *et al.* [2] developed a whole-arm functional neuro-rehabilitation robotic system that consisted of a shoulder-elbow robot (MIT-MANUS), a wrist robot and a hand robot. They proved that the movement therapy had a significant and measurable impact on neurorecovery following injury and effective movement therapy. By coupling models for human arm movement with haptic interfaces and virtual reality technology, Coote *et al.* [3] designed a Gentle/s system that could provide robot-mediated motor tasks in a three dimensional space. Hesse *et al.* [4-5] designed a Bi-Manu-Track robotic arm trainer (AT) to enable bilateral passive and active practice of forearm and wrist movement. They showed that the use of simple devices makes possible intensive training of chronic post stroke patients with positive results in terms of reduction in spasticity, easier hand hygiene, and pain relief. Colombo *et al.* [6] designed a wrist robot and a shoulder-elbow robot that improved the motor outcome and disability of chronic post-stroke patients. Ju *et al.* [7-8] designed an arm-like rehabilitation robot and a forearm torque measurement system. The robot could guide the upper limbs of subjects in linear and circular movements under predefined external force levels and could apply a desired force along the tangential direction of the movements. The forearm torque measurement system could detect and quantify the synergy patterns of the stroke patients during the planar circular movements. Nef *et al.* [9] designed a semi-exoskeleton robot (ARMin) that could support arm therapy related to daily living activities.

In developing rehabilitation robot there is a need for online evaluation of passive joint stiffness, muscle tone or spasticity. Li *et al.*[10] recorded torque and electromyographic (EMG) responses of extrinsic finger flexors subjected to constant-velocity rotation of the metacarpophalangeal (MCP) joints of affected hand. They proved that finger flexor hypertonia is primarily of neural origin, and that it reflects spindle receptor firing properties. Ju *et al.* [11] developed a spasticity measurement system for on-line quantification of the stretch reflex of paretic limbs. They used different constant stretch velocities in a ramp-and-hold mode to elicit the stretch reflex of the elbow joint in spastic subjects and found an index: averaged stretch reflex torque (ASRT) to quantifying the spastic hypertonia. Lin *et al.* [12] developed a pendulum test system for estimating the degree of spasticity of the elbow of the strokes. They used an optimization technique to estimate parameters of the biomechanic model of the elbow as indicators of spasticity. Zhang *et al.* [13] developed an intelligent stretching device to treat the spastic/contracture ankle of neurologically impaired patients. The device can be used to evaluate treatment outcome quantitatively in multiple aspects, including active and passive range of motion (ROM), joint stiffness and viscous damping and reflex excitability.

In our previous research, the shoulder-elbow robot and the wrist robot were not integrated. From our clinical observation, one of the synergy patterns of the stroke patients was the involuntary pronation/supination of forearm while they extended or flexed their elbow joints. A rehabilitation robot which combines shoulder-elbow and wrist might improve stroke patient's synergy patterns. In our previous study, an arm-like rehabilitation robot was developed for neuro-rehabilitation of shoulder and elbow [7]. The old robot is oversized and overweight for clinical applications. Therefore we built a new smaller arm-like robot on top of worktable and the rehabilitation of upper limb has to be extended to forearm. The scope of the current study was confined to construct a robotic system specialized for the rehabilitation of forearm. The robot should be able to assist

P.-C. Kung and M.-S. Ju are with the Department of Mechanical Engineering, National Cheng Kung University, Tainan 70101, Taiwan, R.O.C. (e-mail: n1893123@ccmail.ncku.edu.tw, msju@mail.ncku.edu.tw).

C.-C. K. Lin is with the Department of Neurology, National Cheng Kung University Hospital, Tainan 70101, Taiwan, R.O.C..

the subjects in performing both passive and active forearm pronation/supination subjected to specified loads. The goals of current work are three folds: (1) to develop the forearm robot and its control system, (2) to develop treatment movements plan and (3) performance analyses.

II. METHODS

A. Experimental Setup

The forearm rehabilitation robot consisted of a rotational mechanism, a motion controller, a position and custom-made torque sensors, and a personal computer. This forearm robot was installed on an arm-like rehabilitation robot (Fig. 1).The forearm of the subject was positioned by an expandable clamp in side a rotating drum. The weight of the forearm was supported by the clamp and the drum. A pinion matched with the gear of the rotating drum with a gear ratio of 1:10. The pinion shaft was connected to an AC servo motor with a torque capacity of 4.8 Nm. The other end of the pinion shaft reducer was connected to a custom-made torque sensor. Four strain gages formed a full-bridge circuit on the shaft of the sensing unit which can detect the reactive torque from the subject's arm. Through this mechanism, the forearm of the subject could be manipulated by the rehabilitation robot and the subject can perform pronation and supination movements. The angle of the forearm was recorded by an encoder on the motor and the torque between the forearm and the motor was measure by the torque sensor. The signals were transferred to a personal computer through an A/D board (PCI-6036E, National Instruments, http://ni.com). Within each sampling interval the control signal was computed and, a command was sent to the motor drive by a D/A board (PCI-6731, National Instruments, http://ni.com), and drove the rehabilitation robot to move through the desired trajectory.

B. Treatment Movements

Two types of movements were designed in this research, i.e., passive and active movements. The passive movement meant that the subject was asked to relax his forearm and the robot guided the forearm to complete the movement. Under this mode, the muscle mechanics of the patient's forearm could be evaluated and the joint stiffness of forearm rotation could be estimated. The main function of the passive movements was to reduce the muscle tone of the forearm and increase the ROM. In the active mode, subjects had to move actively along a planned trajectory and the robot applied either a resistant or an assistant torque. It is believed that active movements could help patients to increase muscle power. Two treatment trajectories, i.e., seesaw-like and ramp-and-hold trajectories, were performed in this study. The trajectories were designed to mimic the facilitation techniques of the physical therapists. The seesaw-like trajectory [Fig. 2(a)] was used in both modes. The robot could cyclically stretch the forearm of the subject. An adjustable small angle increment was added after a complete cycle was done. Once the angle reached the full range, the forearm was held at that position for a pre-defined period and then was returned to the initial position. The ramp-and-hold trajectory [Fig. 2(b)] was similar to a conventional continuous passive movement (CPM). In the active mode, both the planed and the actual trajectories were projected on the screen and the subjects were asked to follow the trajectory by himself or herself. The whole process was similar to a game and could increase the incentive of participation. The velocity and the holding time in both trajectories could be adjusted individually.

(a)

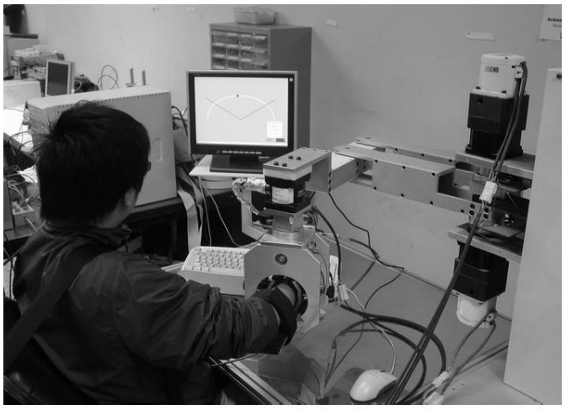

(b)

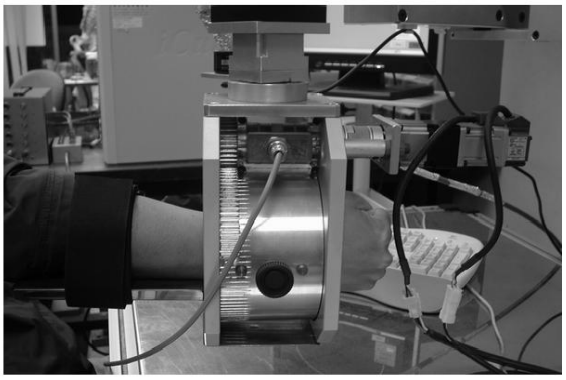

Fig. 1. Photograph of the robot-aided rehabilitation system with a subject (a) and zooming in of the forearm rehabilitation robot part.

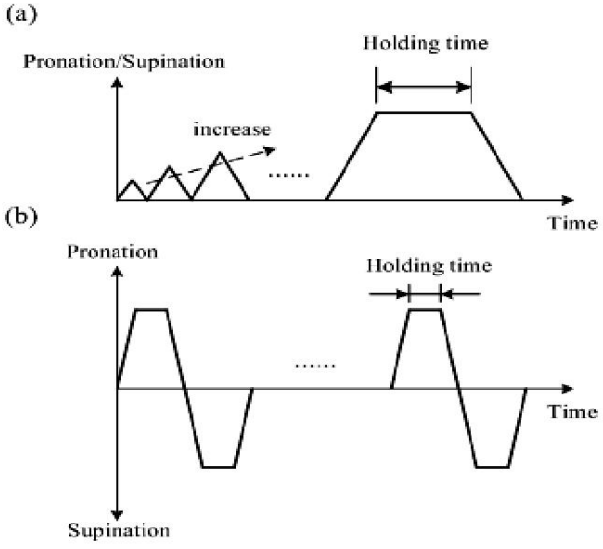

Fig. 2. (a) Seesaw-like trajectory was under passive movements. (b) Ramp-and-hold trajectory was under passive and active movements.

C. Control Strategies

Two control strategies were implemented for the movement control of forearm rotation. In the passive mode, a position fuzzy logic controller [Fig. 3(a)] was adopted and the robot was controlled to stretch the forearm to perform pronation and supination. In the active mode, a fuzzy logic tuned torque controller [Fig. 3(b)] was used to generate the assistant and resistant torque. Both the position and torque controls were implemented in digital control system and the sampling interval (Δt) was 0.02 second.

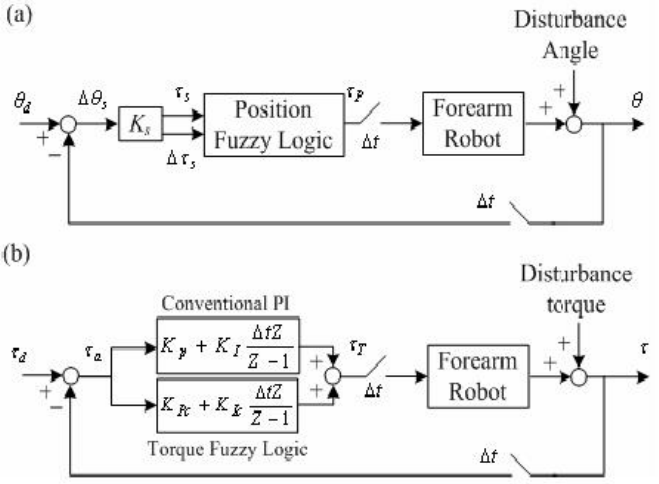

Fig. 3. (a) Block diagram of the position control. (b) Block diagram of the torque control.

In the passive control mode, the stretch position error was transformed into the equivalent torque (τ_s) by a predefined stiffness constant (K_s), i.e.,

$$\tau_s = K_s \cdot \Delta\theta_s \tag{1}$$

where $\Delta\theta_s$ was the stretch position error in one sampling period. τ_s and $\Delta\tau_s$ were the inputs to the fuzzy logic controller and they represented error and error change. In the fuzzification process, input (τ_s and $\Delta\tau_s$) were scaled and mapped to the five triangle-shaped membership functions [Fig. 4(a)], namely, large negative (LN), small negative (SN), zero (ZE), small positive (SP), and large positive (LP). One membership degree was mapped for each scaled input and membership function combination. Then, each combination of mapped inputs (E and EC) activated one control action (B_i, where i, standing for LN, SN, ZE, SP, LP, was ith activated control function) according to the inference rule table [Fig. 4(b)]. We set B_i as the value at the center of base of corresponding membership function (e.g., -1 for SN) and w_i as the minimum of the membership degree of E and EC [Fig. 4(c)]. The output of the fuzzy logic was obtained in the defuzzification process by using the center-of-gravity method

$$\tau_p = \frac{\sum_{i=1}^{n} w_i \cdot B_i}{\sum_{i=1}^{n} w_i} \tag{2}$$

where τ_p was the final output of the position fuzzy controller and i indexed all the combinations of activated control actions from the rule table [Fig. 4(b)].

(a)

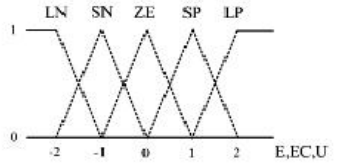

(b)

E \ EC	LN	SN	ZE	SP	LP
LN	LN	LN	LN	LN	LN
SN	LN	SN	SN	ZE	ZE
ZE	SN	SN	ZE	SP	SP
SP	ZE	ZE	SP	SP	LP
LP	LP	LP	LP	LP	LP

(c)

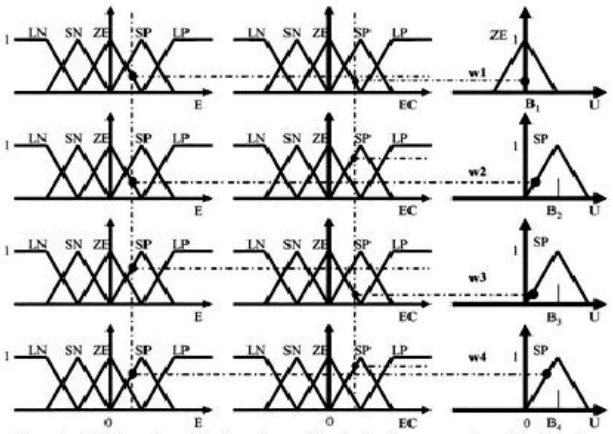

Fig. 4. (a) Membership function, (b) the inference rule table for the position controller, and (c) the fuzzy inference, or decision process. Five membership functions: LN: large negative (left thick line); SN: small negative (left dashed line); ZE: zero (solid line); SP: small positive (right dashed line); and LP: large positive (right thick line) were constructed, where E was the input. Error and error change were projected to the membership function axis, respectively. Projected result (E_1 and E_2) and the corresponding membership degrees were obtained. Then, the inference rule determined B_i (the output of the fuzzification process), where i = LN, SN, ZE, SP, and LP.

In the active control mode, we combined a conventional linear PI (proportional-integral) controller and a fuzzy PI tuner. The function of the fuzzy PI tuner was to compensate the nonlinear dynamics (joint friction) of the robot and the unknown disturbing torque from the subject. τ_a and $\Delta\tau_a$ were fed to the fuzzy PI tuner. The fuzzy PI tuner, having five membership functions in both input and output similar to the position controller described above, had separate fuzzy logics for P and I parts, and each operated in a similar way as in the position controller. The output from the fuzzy logic controller (K_{Pc} for P part and K_{Ic} for I part) were linearly added to the conventional PI controller,

$$\tau_T(l) = [K_P + K_{Pc}(l)] \cdot \tau_a(l) + [K_I + K_{Ic}(l)] \cdot \sum_{m=1}^{n} \tau_a(m)\Delta t \tag{3}$$

$$l = 1, 2, \ldots, n$$

where K_P and K_I were the gains for the conventional PI controller, and τ_T was the final output of the torque control. The maximal values of K_{Pe} and K_{Ie} were set to be the same value as K_P and K_I, respectively.

The whole controller was programmed by using VB (visual basic) language under the Microsoft Windows environment in a personal computer.

D. Safety

Safety measures were implemented both in software and hardware levels. The robot stopped when the movement magnitude or velocity exceeded the predefined limits and the experimenter could stop the robot with an interruption command at any time. Two optical limit switches were employed to define the range of movement of the robot. The robot could also be stopped by shutting down the power supply with an emergency button by the patient or the physical therapist.

III. RESULTS AND DISCUSSION

In this preliminary report, three normal subjects (N1-N3) were recruited. Fig. 5 showed the results of subject N1 performing the seesaw-like trajectory and the ramp-and-hold trajectory in passive mode. In the seesaw-like trajectory the robot increased 5° to the movement range in each cycle and stretched the forearm until it reached 50°. With a ramping velocity of 10°/s and a holding time of 5s, the RMSE (root mean square error) of the tracking in pronation and supination directions were 0.85° and 0.77°, respectively. For the ramp-and-hold trajectory, the forearm of the subject was alternatively pronated and supinated by the robot for 50°. With a ramping velocity of 10°/s and a holding time was 5s, the RMSE of tracking was 0.80° for repeated 5 cycles of movements. The result showed that, under the passive movement, the robot could guide the forearm to pronate/supinate along the desired trajectory. This procedure might increase the ROM in stroke patients in future work.

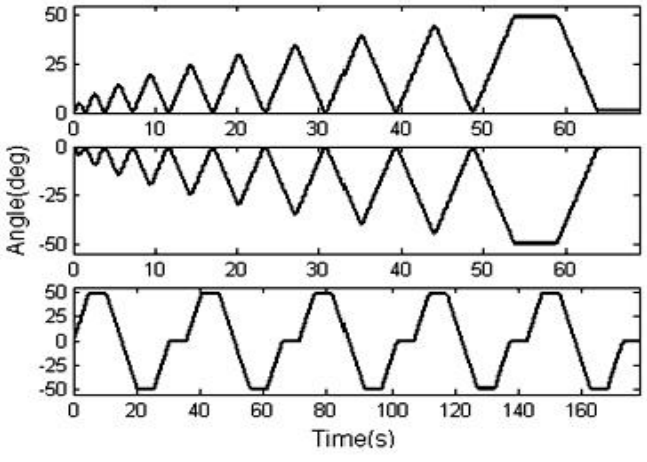

Fig. 5. The subject (N1) performed the seesaw-like trajectory and the ramp-and-hold trajectory under passive movements. The positive angle stand for pronation and negative angle stand for supination. The thin line is the desired trajectories and the thick line is the actual movement trajectories.

Fig. 6 showed the average torque vs. angle curves of dominant and non-dominant arm of 3 subjects under passive mode test. Shown in From Fig. 5 robot-stretched forearm was held for 5 seconds at 50, -50 and 0 degree under ramp-and hold trajectory. The value of torque keeps changing in this period, so spikes appear at 50,-50, 0 degree in Fig. 6. One can observe that the difference between dominant and non-dominant arm is more prominent for subject N1 than the other subjects. When the stretching velocity was very close to zero, the torque-angle curve could be used to evaluate the passive joint stiffness. On the other hand, the muscle tone and spasticity could be estimated from these relationships if the stretching velocity was increased to higher values. Fig. 7 showed the torque-angle relationship of N1's dominant arm in passive mode. Two straight lines were fitted to the torque-angle curve, one for increasing angle and the other for decreasing angle. The slope of the straight line is value of the passive joint stiffness. The results of the dominant and non-dominant of all tested forearms are summarized in Fig. 8. Subject N1 had statistically significant ($t_{18,0.975}$=2.101) difference on dominant and non-dominant side. The other two subjects did not have different passive joint stiffness on dominant and non-dominant sides in statistical significance. Although only three normal subjects were recorded, more clinical trials will be conducted in the future. By using higher stretching velocity the subject's muscle tone or spasticity might also be estimated by the robot.

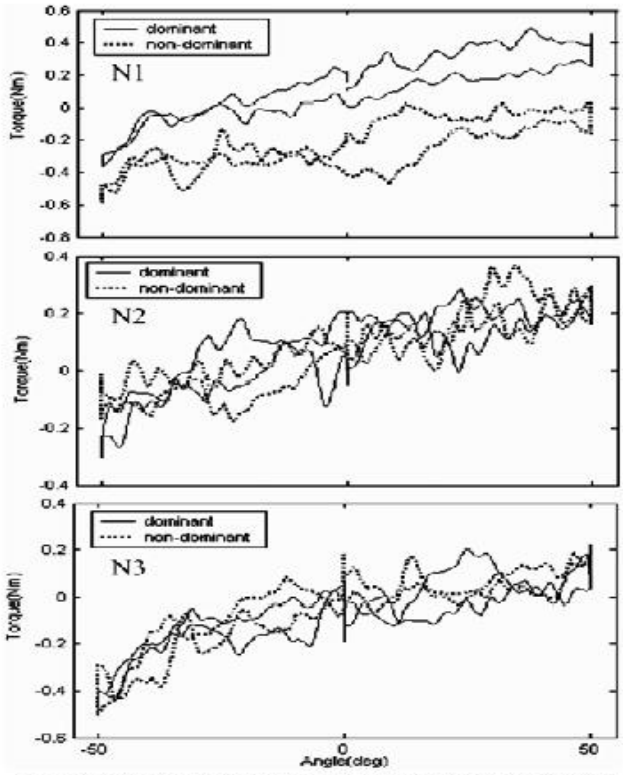

Fig. 6. Showed the relationships between the torque and angle of the dominant and non-dominant arm when the robot stretched the subjects. The positive angle stand for pronation and negative angle stand for supination.

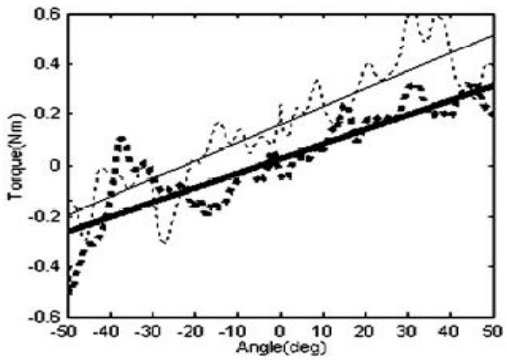

Fig. 7. The fitted of the torque-angle curve of N1's dominant arm in passive mode.

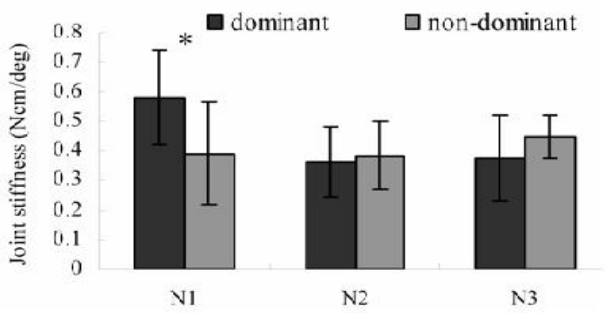

Fig. 8. Showed the passive joint stiffness of the subject's forearm and the statistics propertys.

Fig. 9 showed the performance of subject N1 in the active mode. In this mode, the robot applied a constant load to the subject's forearm while the subject performed active movement. Fig. 9(a) showed the condition when no load (0 Nm) was applied and the RMS torque error was 0.042Nm. Fig. 9(b) showed the condition of an assistant torque of 0.3Nm and it resulted in a RMS torque error of 0.046Nm. Fig. 9(c) showed the condition of a resistant torque of -0.5Nm and it resulted in a RMS torque error of 0.047Nm. The results revealed that in active mode the robot was capable of maintaining constant assistant or resistant torque. The results demonstrated that the control algorithm was successful since only small tracking torque errors were observed in these tests. It is our expectation that, in the future, this procedure could increase the muscle power of the patients.

IV. CONCLUSION

A forearm rehabilitation robot was designed and two control modes and two therapeutic movements were realized and tested on three able-bodied subjects. The preliminary results showed that, in the passive mode, the robot can successfully guided the forearm along the desired trajectory and, in the active mode, the robot could apply and maintain a specified torque during the movement. Ongoing work is to evaluate the effectiveness of this robot to assisting the rehabilitation of stroke patients. Furthermore the forearm robot will be integrated with the shoulder-elbow robot to study the synergy pattern in stroke patients.

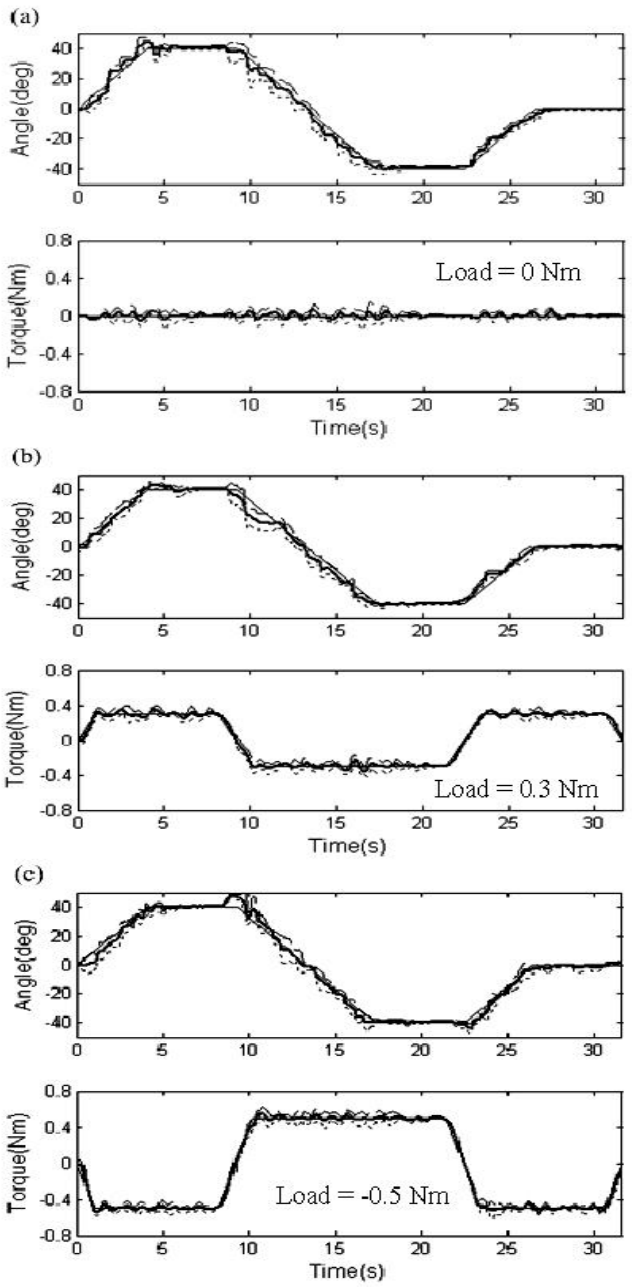

Fig. 9. The subject (N1) performed the ramp-and-hold trajectory under active movements and repeated 5 times. The thin lines are the mean of the desired angle and torque trajectories. The thick lines are the mean of the actual angle and torque trajectories. The dashed lines are one positive and negative standard deviation of the mean, respectively.

V. ACKNOWLEDGMENTS

The research is supported by the Ministry of Economic Affairs, R.O.C., under the contract 95-EC-17-A-19-S1-053.

REFERENCES

[1] P. S. Lum, C. G. Burgar, P. C. Shor, et al., "Robot-Assisted Movement Training Compared with Conventional Therapy Techniques for the Rehabilitation of Upper-limb Motor Function After Stroke", Arch. Phys. Med. Rehabil., vol. 83, pp.952-959, 2002.

[2] H. I. Krebs, N. Hogan, "Therapeutic Robotics: A Technology Push", Proceedings of the IEEE, vol. 94, no. 9, September 2006.

[3] S. Coote, E. K. Stokes, "Robot Mediated Therapy: Attitudes of Patients and Therapists Towards the First Prototype of the GENTLE/s System", Technology and Disability, 15, 27-34, 2003.
[4] S. Hesse, G. Schulte-Tigges, M. Konrad, A. Bardeleben, C. Werner, "Robot-Assisted Arm Trainer for the Passive and Active Practice of Bilateral Forearm and Wrist Movements in Hemiparetic Subjects", Arch. Phys. Med. Rehabil., vol. 84, June, 2003.
[5] S. Hesse, C. Werner, M. Pohl, S. Rueckriem, J. Mechrholz, M. L. Lingnau, "Computerized Arm Training Improves the Motor Control of the Severely Affected Arm after Stroke", Stroke, September 2005.
[6] R. Colombo, F. Pisano, S. Micera, A. Mazzone, C. Delconte, M. C. Carrozza, P. Dario, G. Minuco., "Robotic Techniques for Upper Limb Evaluation and Rehabilitation of Stroke Patients", IEEE Transactions on Neural Systems and Rehabilitation Engineering, vol. 13, no. 3, pp. 311-324, 2005.
[7] M.-S. Ju, C.-C. K. Lin, D.-H. Lin, I.-S. Hwang, S.-M. Chen, "A Rehabilitation Robot with Force-Position Hybrid Fuzzy Controller: Hybrid Fuzzy Control of Rehabilitation Robot", IEEE Transactions on Neural Systems and Rehabilitation Engineering, vol. 13, no. 3, pp. 349-358, 2005.
[8] B.-C. Kung, M.-S. Ju, C.-C. K. Lin, S.-M. Chen, "Clinical Assessment of Forearm Pronation/Supination Torque in Stroke Patients", Journal of Medical and Biological Engineering, vol. 25, no. 1, pp. 39-43, 2005.
[9] T. Nef, R. Riener, "ARMin-Design of a Novel Arm Rehabilitation Robot", IEEE 9th International Conference on Rehabilitation Robotics, June 28 - July 1, Chicago, IL, USA, pp. 57-60, 2005.
[10] S. Li, D. G. Kamper, W. Z. Rymer, "Effects of Changing Wrist Position on Finger Flexor Hypertonia in Stroke Survivors", Muscle Nerve, vol. 33, pp. 183-190, 2006.
[11] M.-S. Ju, J.-J. J. Chen, H.-M. Lee, T.-S. Lin, C.-C. Lin, Y.-Z. Huang, "Time-course analysis of stretch reflexes in hemiparetic subjects using an on-line spasticity measurement system", J Electromyogr & Kinesiol, vol. 10, pp. 1-14, 2000.
[12] C.-C. K. Lin, M.-S. Ju, C.-W. Lin, "The pendulum test for evaluating spasticity of the elbow joint", Arch Phys Med Rehabil, vol. 84, pp. 69-74, 2003
[13] L.-Q. Zhang, S. G. Chung, Z. Bai, D. Xu, E. M. T. van Rey, M. W. Rogers, M. E. Johnson, E. J. Roth, "Intelligent Stretching of Ankle Joints With Contracture/Spasticity", IEEE Transactions on Neural Systems and Rehabilitation Engineering, vol. 13, no. 3, pp. 349-358, 2005.